

PROPERTIES OF LITHIUM–ALUMINUM–COBALT–MANGANESE OXIDE NANOCOMPOSITES FORMED BY CHEMICAL COPRECIPITATION

Chen–Feng Kao and Kao–Heng Liu

Department of Chemical Engineering, National Cheng Kung University, Tainan, 70101, TAIWAN

Introduction

Kao and Wu have studied the preparation and properties of the lithium–manganese oxide ceramic matrix by various processes[1] and the lithium–manganese–vanadium oxide ceramic matrix composites by chemical coprecipitation[2].

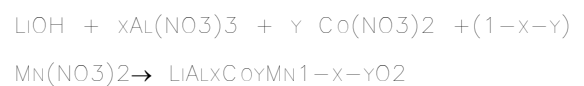
Aluminum is very light metal and its electrode potential is high. Therefore it becomes a very important material in battery.

Kumagai et al. [3] have investigated the physical and electrochemical characterization of quaternary Li–Mn–V–O spinel as positive materials for rechargeable lithium batteries.

In this study, the particle size and electrical properties of the lithium–aluminum–cobalt–manganese oxide particle by chemical coprecipitation were determined.

Experimental

Fig. 1 Flow chart for experiment of $\text{LiAl}_x\text{Co}_y\text{Mn}_{1-x-y}\text{O}_2$



WHERE $x = 2/3, 1/3$.

THE CHEMICALS USED WERE ALL OF HIGH PURITY. LiOH , $\text{Al}(\text{NO}_3)_3$, $\text{Co}(\text{NO}_3)_2$ AND $\text{Mn}(\text{NO}_3)_2$ WERE USED AS THE STARTING REAGENTS OF $\text{Li}(\text{I})$, $\text{Al}(\text{III})$, $\text{Co}(\text{II})$ AND $\text{Mn}(\text{II})$, RESPECTIVELY.

THE MOLE RATIOS OF $\text{LiAl}_x\text{Co}_y\text{Mn}_{1-x-y}\text{O}_2$ ARE 1:1/3:1/6:1/2, 1:1/3:1/3:1/3, 1:1/3:1/2:1/6, 1:2/3:1/9:2/9 AND 1:2/3:2/9:1/9, RESPECTIVELY.

Result and Discussion

Lithium Aluminum Cobalt Manganese Oxide Nanocomposites

FTIR

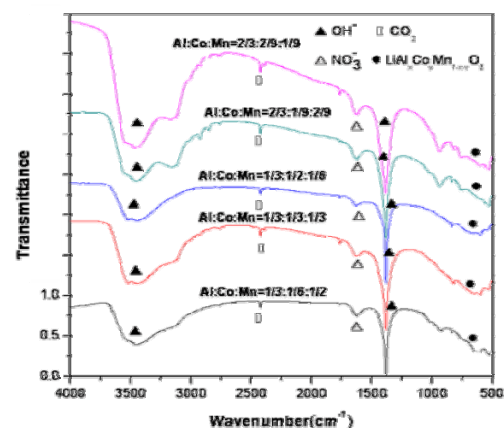


Fig. 2 FTIR spectra of

$\text{LiAl}_x\text{Co}_y\text{Mn}_{1-x-y}\text{O}_2$ precursors dried at 150°C for 24h

That there are peaks at $1210\text{--}1570\text{ cm}^{-1}$ and $2690\text{--}3750\text{ cm}^{-1}$ for OH-bending,

around $1570\text{--}1760\text{ cm}^{-1}$ for NO_3^- , and at $500\text{--}950\text{ cm}^{-1}$ for spinel [4].

TGA/DTA and XRD analyses of coprecipitated powder

There is a weight loss in the $273\text{--}473\text{ K}$ for the Li-Al-Co-Mn oxide particle in TGA/DTA, owing to the vaporization of the water in the precursor from absorption heat.

There is also a weight loss in $473\text{--}593\text{ K}$, because nitrate reacted into nitrogen oxide.

In the vicinity of 593 K the OH- reacted into water and the vaporization of water from absorption heat.

There are clear peaks from the XRD pattern of the powder in coprecipitation of Li-Al-Co-Mn oxide particle at 423 K for 24 h. It is obvious that there is a crystal structure of $\text{LiAl}_x\text{Co}_y\text{Mn}_{1-x-y}\text{O}_2$.

Heated to 1273 K , the product of $\text{LiAl}_x\text{Co}_y\text{Mn}_{1-x-y}\text{O}_2$ is complete for the reaction.

Fig. 3 SEM of $\text{LiAl}_x\text{Co}_y\text{Mn}_{1-x-y}\text{O}_2$. That there is a clear phenomenon of agglomeration from SEM. This phenomenon is attributed to van der Waals forces between molecules, the absorption of vapor and the defect for the surface of the grain or having no balance in electricity to produce aggregation and tendency of adsorptive outer substances [5,6]

Particle Size Distribution of $\text{LiAl}_x\text{Co}_y\text{Mn}_{1-x-y}\text{O}_2$

The average particle sizes of $\text{LiAl}_{2/3}\text{Co}_{1/9}\text{Mn}_{2/9}\text{O}_2$ and $\text{LiAl}_{1/3}\text{Co}_{1/2}\text{Mn}_{1/6}\text{O}_2$ are 0.421 and $0.459\text{ }\mu\text{m}$, respectively from their particle size distribution. Owing to the radius of cobalt is larger than that of aluminum, the average particle size of $\text{LiAl}_{1/3}\text{Co}_{1/2}\text{Mn}_{1/6}\text{O}_2$ is larger than that of $\text{LiAl}_{2/3}\text{Co}_{1/9}\text{Mn}_{2/9}\text{O}_2$.

XRD Analysis

It is obvious from Figure 4 that at 800°C the structure of the lithium aluminum cobalt manganese oxide

appeared, and there was no change until 1000°C. Some Mn₂O₃ existed at 800°C and disappeared at 1000°C. Therefore the optimal condition for preparing the lithium aluminum cobalt manganese oxide is at 1000°C for 6 h.

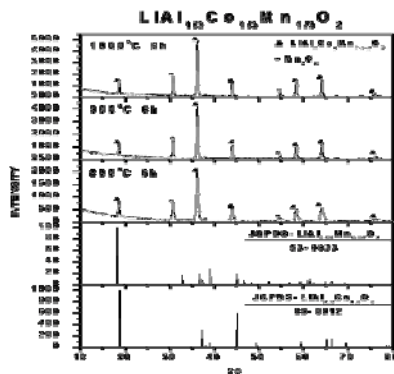


Fig. 4 XRD of LiAl_{1/3}Co_{1/3}Mn_{1/3}O₂ Superconducting Quantum Interference Device (SQUID)

The magnetic susceptibility of the sintered lithium aluminum cobalt manganese oxide particle as a function of temperature by SQUID. The magnetic susceptibility decreases with increasing temperature. The magnetic intensity, I, with magnetic strength, H, is written as $I = XH$, where X is magnetic susceptibility. And susceptibility is proportional to $1/T$ as C/T [7,8].

SQUID was used to measure $1/X$ vs. T. The results for the various sintered are paramagnetism.

Measurement of Resistivity for the Sintered Body in Air at Room Temperature

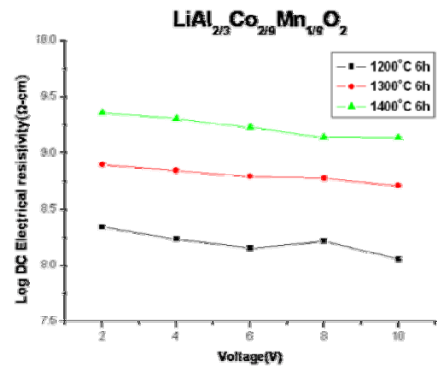


Fig. 5 DC electrical resistivity of LiAl_{2/3}Co_{1/9}Mn_{2/9}O₂ bodies sintered at 1200,1300 and 1400C for 6h

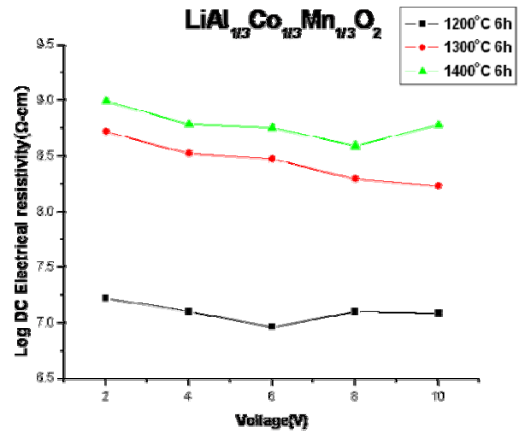


Fig. 6 DC electrical resistivity of LiAl_{1/3}Co_{1/3}Mn_{1/3}O₂ bodies sintered at 1200, 1300 and 1400C for 6 h

Measurement of Dielectric Constant for the Sintered Body

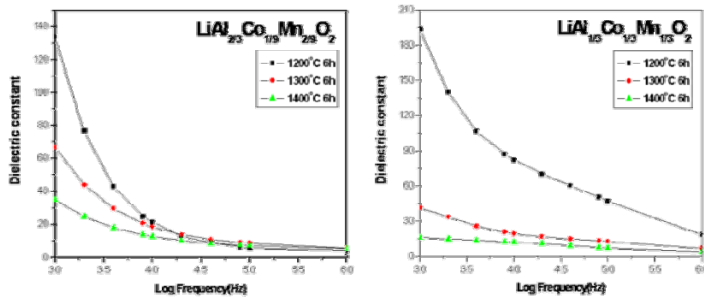


Fig.7 Dielectric constant of $\text{LiAl}_x\text{Co}_y\text{Mn}_{1-x-y}\text{O}_2$

$\epsilon_r = (t_a \cdot c_p) / (\pi r^2 \epsilon_0)$ [9], where t_a is the thickness of the sample, r is the measured radius of the holder, 2.5×10^{-3} m, ϵ_0 is the dielectric constant in air, 8.854×10^{-12} F/m and c_p is the measured capacitance.

That the dielectric constant decreases with increasing frequency. The dielectric constant decreases with increasing sintering temperature. And that the dielectric constant of high aluminum content is less than that of low aluminum content.

Charge and discharge curves of the lithium aluminum cobalt manganese oxide particles

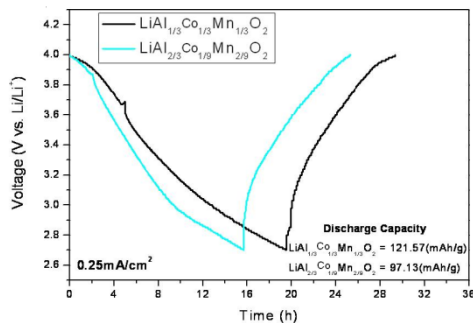


Fig. 8 Charge and discharge curves of the lithium aluminum cobalt manganese oxide

Conclusions

(1) The lithium–aluminum–cobalt–manganese oxide particles, the reactants act the coprecipitant to simplify the reaction procedure and obtain the fine powder at lower calcination temperature of 1273 K.

(2)The uniformities of the particles are better. XRD, SEM and FTIR were used to examine the effect of manganese. When the concentration of manganese ion increases, the absorption strength of the peak of spinel structure in the FTIR patterns decreases, due to the occupation of manganese in the aluminum position.

(3)The charge–discharge curve of the lithium–aluminum–cobalt–manganese oxide particle as a cathode material of the lithium ion battery was also determined.

References

1. Chen–Feng Kao and Ming–Shiou Wu, Preparation and Properties of Lithium–Manganese Oxide Ceramic Matrix by Various Processes, *Fifth International Conference on Composites Engineering*, 457–458(1998).
2. Chen–Feng Kao and Ming–Shiou Wu, Preparation and Characterization of Lithium–Manganese–Vanadium Oxide Ceramic Matrix Composites by Chemical Coprecipitation, *Ceramic Transactions*, 103, 105–123(2000).
3. N. Kumagai, T. Fujiwara and K.

Tanno, Physical and Electrochemical Characterization of Quaternary Li–Mn–V–O Spinel as Positive materials for Rechargeable Lithium Batteries, *J. Electrochem. Soc.*, 143, 1007–1013(1996).

4. P. Kalyani, N. Kalaiselvi, N. G. Renganathan, M. Raghavan, Studies of $\text{LiNi}_{0.7}\text{Al}_{0.3-x}\text{Co}_x\text{O}_2$ solid solutions as alternative cathode materials for lithium batteries, *Mater. Res. Bull.*, 39, 41–54(2004).

5. R.G. Darrie, W. P. Doyle and I. Kirkpatrick, Spectra and Thermal Decomposition of Chromate(VI) of Magnesium, Lanthanum, Neodymium and Samarium, *J. Inorg. Nucl. Chem*, 29, 979–992(1967).

6. G. V. Subba Rao and C. N. R. Rao and J. R. Ferraro, Infrared and Electronic Spectra of Rare Earth Perovskite : Ortho–Chromites, –Manganites, and –Ferrites, *Applied Spectroscopy*, 24, 436(1970).

7. B. D. Cullity, Introduction to magnetic Materials, 85–203, *Addison–Wesley*, 1972.

8. S. Chikazumi and S. H. Charap, Physics of magnetism, 37–109, *John Wiley & Sons*, 1985.

9. A. A. Zaky and R. Hawley, Dielectric Solids, 281, *Dover, N.Y.*, 1970.